# Isomerization and Dissociation in Competition: The Two-Component Dissociation Rates of Methyl Propionate Ions

**Oleg A. Mazyar and Tomas Baer***

*Chemistry Department, University of North Carolina at Chapel Hill, Chapel Hill, North Carolina 27599-3290*

*Received: November 5, 1998; In Final Form: December 30, 1998*

Threshold photoelectron−photoion coincidence (TPEPICO) spectroscopy has been used to investigate the unimolecular chemistry of gas-phase methyl propionate ions. This ion undergoes isomerization to a lower energy enol structure, $CH_3CHC(OH)OCH_3^{\bullet+}$, via two different pathways involving two distonic isomers, $^{\bullet}CH_2CH_2C^+(OH)OCH_3$ and $CH_3CH_2C^+(OH)OCH_2^{\bullet}$. This isomerization reaction is in competition with the direct $CH_3O^{\bullet}$ loss reaction, which leads to two-component dissociation rates of the methyl propionate ions. Detailed modeling of this complex reaction permitted the extraction of the dissociative photoionization threshold for methyl propionate, which at 0 K is 10.83 ± 0.01 eV, as well as the isomerization barrier between the distonic $CH_3CH_2C^+(OH)OCH_2^{\bullet}$ and enol $CH_3CHC(OH)OCH_3^{\bullet+}$ ions of 8.5 kcal/mol (relative to the methyl propionate ion). By combining this with the 0 K heats of formation of methyl propionate and the methoxy radical, we derive a 0 K heat of formation of the product propanoyl ion of 147 kcal/mol. Also measured was the adiabatic ionization energy of methyl propionate, 10.03 ± 0.05 eV.

## Introduction

The complex dissociation dynamics of gas-phase ester ions has been a long-discussed problem in gas-phase ion chemistry. Most of these ions rearrange to more stable isomers prior to dissociation. Several of them undergo competitive dissociation and isomerization reactions leading to two-component unimolecular dissociation rates. Two-component dissociation rates arise when an ion can dissociate rapidly via a simple bond break or isomerize via rearrangement to a lower energy structure. The dissociation rate constant from this lower energy structure will be slow because the activation energy is much higher. A general mechanism can be written as follows:

$$A^+ + B \xleftarrow{k_1} AB^+ \underset{k_3}{\overset{k_2}{\rightleftharpoons}} CD^+ \qquad (1)$$

in which $CD^+$ is a low-energy isomer of $AB^+$. If $k_2 \gg k_1$, all ions rearrange to the $CD^+$ structure prior to dissociation and thus dissociate with a slow rate constant determined by the depth of the potential well of $CD^+$. If, however, $k_1 \gg k_2$, then none of the ions isomerize and the rate will be fast. Now, if $k_1 \approx k_2$, then some ions dissociate rapidly by direct dissociation to $A^+ + B$ while others isomerize and come back much more slowly. Whether the two-component dissociation is observed or not depends very sensitively on the relative barrier heights for direct dissociation (via $k_1$) and isomerization (via $k_2$).

We have already investigated the two-component dissociation dynamics of methyl formate, methyl acetate, and ethyl formate ions by threshold photoelectron−photoion coincidence (TPEPICO) time-of-flight mass spectrometry.[1−3] In the case of methyl formate ions, CO loss proceeds both by fast and slow rates. In this case, a distonic ion $HCOHOCH_2^{\bullet+}$ is the lower energy isomer of the methyl formate ion which determines the slow component of the dissociation. The ionized methyl acetate dissociates by losing $CH_3O^{\bullet}$ and $CH_2OH^{\bullet}$ radicals. The loss of the methoxy radical proceeds both by fast and slow rates, while the lower energy hydroxymethyl radical loss proceeds by only the slow rate. The dissociation of the ethyl formate ion, an isomer of methyl acetate, is also two-component. However, it fragments by a completely different mechanism via the loss of $H^{\bullet}$, $H_2O$, and HCOOH. In both methyl acetate and ethyl formate ions, the lower energy isomers that produce the slow dissociation rates are the enol and distonic ions in which one of the alkyl hydrogen atoms moves to the carbonyl oxygen thereby stabilizing the ion by 10 to 20 kcal/mol.

The methyl propionate ion is another wonderful example of a complex dissociation/isomerization mechanism of ester ions. Unlike the ionized methyl acetate, the methyl propionate ion generates solely the $CH_3O^{\bullet}$ radical.[4,5] The deuterium labeling experiments show that the $CH_3CH_2COOCD_3^{\bullet+}$ ion undergoes extensive H/D randomization.[6] This is possible if two distonic isomers, $^{\bullet}CH_2CH_2C^+(OH)OCH_3$ and $CH_3CH_2C^+(OH)OCH_2^{\bullet}$, as well as the enol ion $CH_3CHC(OH)OCH_3^{\bullet+}$ participate in the unimolecular dissociation/isomerization reaction of the methyl propionate ion. Labeling experiments on the $CH_3CH_2COOCD_3^{\bullet+}$ and $CD_3CH_2COOCH_3^{\bullet+}$ ions demonstrated that the long-lived methyl propionate ions undergo competitive isomerization to both distonic ions, $^{\bullet}CH_2CH_2C^+(OH)OCH_3$ and $CH_3CH_2C^+(OH)OCH_2^{\bullet}$, by the [1,4]-hydrogen shift to the carbonyl oxygen from the acid and alcohol moieties, respectively.[7] The [1,4]-shift of the $\beta$-hydrogen of the acid moiety was found to be the favored rearrangement channel.[7] The double-collision experiments on the $CH_3CH_2COOCD_3^{\bullet+}$ ion, however, showed that the concentration of the $CH_3CH_2COHOCD_2^{\bullet+}$ ions in the reacting mixture must be very small in comparison with the concentration of another distonic ion, $CH_2CH_2COHOCD_3^{\bullet+}$.[5] This disagreement might indicate that the distonic ion $^{\bullet}CH_2CH_2C^+(OH)OCH_3$ is more stable, and the high concentration of this ion in the equilibrated reaction mixture is due to the high density of states associated with this isomer.[8] It should be noted that these two distonic isomers are linked by the low-energy [1,5]-H transfer transition state,[9] which is expected to

10.1021/jp984322p CCC: $18.00 
Published on Web 02/13/1999

be some 7−10 kcal/mol below the $CH_3O^•$ loss dissociation barrier of the methyl propionate ion of 14.5 kcal/mol.[10] Thus, the distonic isomers could be in equilibrium on the microsecond time scale under the experimental conditions of Burgers et al.[5]

The distonic ion $CH_3CH_2C^+(OH)OCH_2^•$ undergoes further [1,4]-hydrogen shift from the α-carbon to the radical site on the alcohol moiety to produce the enol ion of the methyl propionate,$CH_3CHC(OH)OCH_3^{•+}$.[7,11] The long-lived (>0.5 s) methyl propionate ions were found to isomerize to the enol form completely.[11] According to Holmes and Lossing,[12] the enol ion of the methyl propionate lies some 32 kcal/mol below the keto structure and is the global minimum on the potential energy surface (PES) of the ionized methyl propionate. Recently, the 0 K heat of formation of the enol ion of the methyl propionate of 106 ± 2 kcal/mol was derived from the dissociative photoionization threshold for the methyl 2-methyl butanoate,[13] measured by the threshold photoelectron−photoion coincidence (TPEPICO) technique,[14] which is in a good agreement with the value of 105 kcal/mol obtained by converting the Holmes and Lossing 298 K value of 99 kcal/mol.[12] It should be noted that the uncertainty of ±2 kcal/mol was assigned arbitrarily, as it is determined only by the uncertainty of the heat of formation of the methyl 2-methyl butanoate, which was calculated by Holmes and Lossing[12] using simple additivity principles.

Recently, it was suggested that the keto−enol tautomerization of the ionized methyl propionate is associated with a very complicated four-well PES, which involves the methyl propionate ion, two distonic and enol ions.[7,11] This PES suggests that the $CH_3O^•$ loss from the methyl propionate ion may proceed with multicomponent dissociation rates. The TPEPICO technique[14] allows us to verify this. In addition, the RRKM analysis of the dissociation rates extracted from the TPEPICO TOF spectra[8,15] will yield a very accurate value for the 0 K dissociative ionization threshold of the methyl propionate, which cannot be obtained from the traditional threshold photoionization measurements,[10] and thus the 0 K heat of formation of the propanoyl cation. This is in part the purpose of the present paper.

In addition, we will provide an estimation of the energy of the barrier between the distonic $CH_3CH_2C^+(OH)OCH_2^•$ and enol $CH_3CHC(OH)OCH_3^{•+}$ isomers of the methyl propionate ion based on the ratio of the fast and slow dissociation components in the TPEPICO TOF spectra, as well as a complete PES for the isomerization/dissociation reaction of the ionized methyl propionate calculated on the G2 level of theory.[16]

## Experimental Approach

The experimental apparatus has been described previously.[17] Briefly, the room-temperature sample molecules were ionized with vacuum ultraviolet (VUV) light from an $H_2$ discharge lamp dispersed by a 1 m normal incidence monochromator. An electric field of 20 V/cm accelerates electrons and ions in opposite directions. Threshold electrons were selected by a steradiancy[18,19] and hemispherical analyzers (∼30 meV combined photon and electron energy resolution) and detected with an electron multiplier. The resulting ions were detected in coincidence with their corresponding electrons. The time difference between the two detection events determines the ion's time-of-flight (TOF). For each coincidence event, the TOF was electronically converted to a peak height and sorted on a multichannel analyzer. TOF distributions were obtained in 36−48 h.

The experiment involved measuring the product ion TOF distributions. Slowly dissociating ions decay as they are accelerating in the 5 cm long acceleration region. This results in asymmetric TOF distributions from which a dissociation rate can be extracted.

**Ab initio Molecular Orbital Calculations.** To verify the methyl propionate ion isomerization/dissociation mechanism suggested by Leeck et al.[11] and Pakarinen et al.,[7] ab initio molecular orbital (MO) calculations were performed with the Gaussian 94 program.[20] The G2 calculations[16] were carried out on four stable isomers of the methyl propionate ion, including two distonic ions, $^•CH_2CH_2C^+(OH)OCH_3$ and $CH_3CH_2C^+(OH)OCH_2^•$, and the enol ion $CH_3CHC(OH)OCH_3^{•+}$, as well as on four transition states linking them (see Figure 1 and Table 1). The relationship between these structures is shown in Figure 2. Geometries of both the stable isomers and the transition states optimized at the MP2(FULL)/6-31g* level of theory are shown in the Figure 1. Bond lengths are given in angstroms and bond angles in degrees.

Vibrational frequencies and zero-point vibrational energies (ZPE) of the $C_4H_8O_2^{•+}$ structures were calculated at the unrestricted Hartree−Fock level of theory using the split-valence 6-31g* basis set, which includes a set of polarization functions for all non-hydrogen atoms. Harmonic vibrational frequencies and ZPEs were corrected by factors 0.8929 and 0.9135, respectively, to take into account the fact that at the UHF/6-31g* level the fundamental frequencies are overestimated by ∼10%[21,22] (see Tables 1 and 2).

The G2 energies of the methyl propionate ion, its isomers, and the transition states linking them are listed in Table 1. The spin contaminations, $\langle S^2 \rangle$, calculated at the MP2(FULL)/6-31g* level of theory, were within an acceptable range and close to the value of 0.76 for the stable isomers but were found to be slightly higher (from 0.774 to 0.794) for the transition states (see Table 1). For comparison, Table 1 also shows the MP2(FULL)/6-31g* energies of the $C_4H_8O_2^{•+}$ structures. It is interesting that the MP2 calculations on the stable structures agreed very well with the G2 calculations. The relative energies of the two distonic ions, B and C, and the enol isomer D (relative to the methyl propionate ion A) calculated at the MP2/6-31g* + ZPE level of theory agree within 1.6 kcal/mol with those calculated at the G2 level (see Table 1). The difference between the relative energies of the transition states calculated at the MP2 and G2 levels, however, is more significant; the MP2 theory predicts transition state energies that are 2−4 kcal/mol higher than the G2 theory calculations.

The methyl propionate ion (structure A in Figure 1) can rearrange to two different distonic isomers $^•CH_2CH_2C^+(OH)OCH_3$ (structure B) and $CH_3CH_2C^+(OH)OCH_2^•$ (structure C) via the transition states TSAB and TSAC, representing five-centered activation complexes (see Figures 1 and 2).[7] The G2 calculations support the recent findings of Pakarinen et al.[7] that the [1,4]-transfer of the β-hydrogen of the acid moiety to the carbonyl oxygen in the methyl propionate ion (see TSAB in Figure 1) requires some 4 kcal/mol less than the [1,4]-hydrogen shift to the carbonyl oxygen from the alcohol moiety (TSAC in Figure 1).

Isomerization of the distonic ion B to the distonic ion C via the [1,5]-hydrogen transfer from the methoxy group to the radical site on the acid moiety involves a transition state TSBC that lies some 3.5 kcal/mol below the transition structure TSAC (see Table 1). The distonic ion C, however, is not formed exclusively via the reaction path involving two low-energy transition states, TSAB and TSBC (see Figure 2). In fact, this process is in competition with the direct generation of the isomer C from the methyl propionate ion, A, via the transition structure TSAC.[7] Despite the low energies of the transition states TSAB

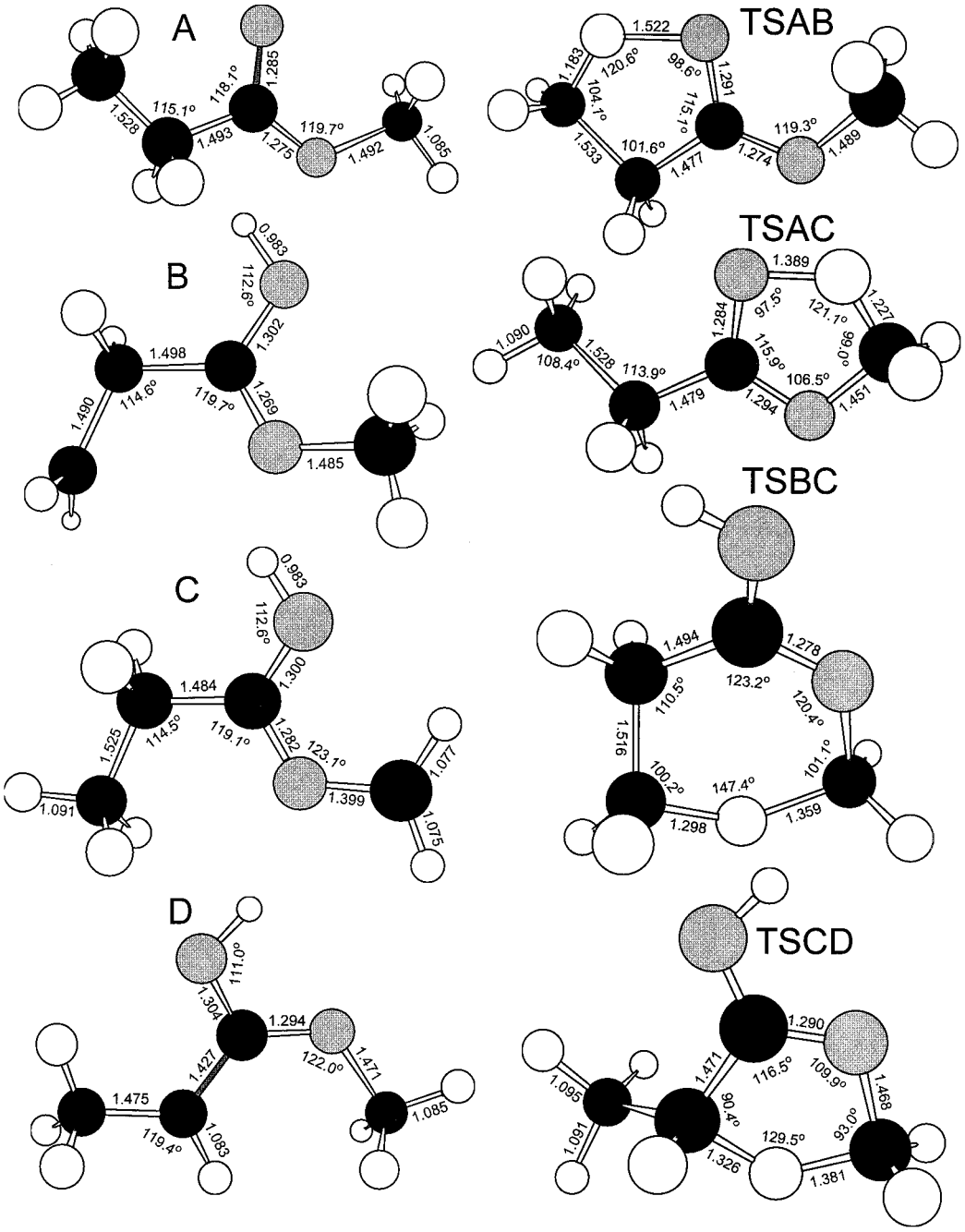


**Figure 1.** MP2(FULL)/6-31g* optimized geometries of the various isomers of the methyl propionate ion and the transition states linking them.

and TSBC, the rate of formation of the isomer C via two consecutive reactions A → B and B → C is limited (from the RRKM[8] point of view) by the high density of states associated with the distonic ion B. At the same time, the reverse reaction, C → B dominates over C → A, as the RRKM expressions for the rates of these reactions include the density of states of the same isomer C.[8]

The distonic ion C undergoes further isomerization to the enol ion of the methyl propionate (structure D in Figure 1) via a [1,4]-hydrogen shift from the α-carbon of the acid moiety to the radical site on the alcohol moiety (TSCD in Figure 1). This rearrangement requires 8.7 kcal/mol of energy (with respect to the methyl propionate ion A). This is some 1.5 kcal/mol higher than the TSBC and 2 kcal/mol higher than the TSAB (see Table 1). According to the ab initio MO calculations, only the transition state TSAC has higher energy than the TSCD, but it is bypassed by the lower energy transition state TSAB (see Figure 2). Thus, the isomerization reaction C → D represents the rate-limiting step in the rearrangement of methyl propionate ion A to its enol form D (see Figure 2). It should be noted that the direct rearrangement of the methyl propionate ion A to the enol ion D via the [1,3]-hydrogen transfer requires about 30 kcal/mol[23] and thus is ignored in this study.

To model the dissociation rates with RRKM theory, it is helpful to consider the essential features of the ion's potential energy surface (PES) shown in Figure 2. The A potential well is not very deep so that the lifetime of the ion in its keto conformation will be very short. The keto isomer A readily rearranges to the distonic structures B and C, which in their turn reach partial equilibrium between themselves as well as with the structure A before the isomerization to the lowest energy enol isomer D. Thus, the keto structure A and two distonic isomers B and C can be treated as a single potential well. The resulting two-well dissociation model is shown in

**TABLE 1: Calculated Energies and ZPE of Ions, Transition States, and Dissociation Products**

| | ZPE,[a] HF/6-31g* (hartrees) | MP2(FULL)/6-31g* (hartrees) | G2 (hartrees) | $\langle S^2 \rangle$ | $E_{rel}$, MP2 (kcal/mol) | $E_{rel}$, G2 (kcal/mol) |
|---|---|---|---|---|---|---|
| species | | | | | | |
| A | 0.126045 | −306.3963858 | −306.815398 | 0.76 | 0 | 0 |
| B | 0.124663 | −306.420553 | −306.8381763 | 0.762 | −15.96 | −14.29 |
| C | 0.125072 | −306.4184688 | −306.8367305 | 0.766 | −14.42 | −13.39 |
| D | 0.126648 | −306.4407247 | −306.8572162 | 0.76 | −27.48 | −26.24 |
| TSAB | 0.121503 | −306.3773641 | −306.8047204 | 0.774 | 9.33 | 6.70 |
| TSAC | 0.120895 | −306.3687242 | −306.7982788 | 0.785 | 14.41 | 10.74 |
| TSBC | 0.121388 | −306.3759351 | −306.803898 | 0.788 | 10.16 | 7.22 |
| TSCD | 0.121116 | −306.374535 | −306.8015748 | 0.794 | 10.89 | 8.67 |
| products | | | | | | |
| $CH_3CH_2CO^+$ | 0.079268 | −191.6682982 | −191.9131991 | | | |
| $CH_3O^\bullet$ | 0.040280 | −114.6930928 | −114.8675387 | 0.758 | | |
| products | | | | | 18.24 | 21.75 |

[a] To be scaled by 0.9135.[21,22]

**TABLE 2: Vibrational Harmonic Frequencies Used in This Study,[a] $cm^{-1}$**

| | |
|---|---|
| A(neutral) | 48, , 136, 161, 199, 217, 319, 426, 565, 640, 793, 845, 950, 1012, 1082, 1092, 1159, 1192, 1235, 1255, 1377, 1407, 1440, 1458, 1464, 1467, 1470, 1474, 1797, 2874, 2879, 2902, 2905, 2933, 2946, 2974, 2989 |
| A | 11, 106, 154, 174, 226, 272, 398, 534, 542, 773, 797, 838, 954, 1058, 1091, 1137, 1172, 1249, 1300, 1333, 1405, 1409, 1428, 1441, 1457, 1463, 1463, 1573, 2882, 2889, 2921, 2929, 2958, 2969, 3030, 3065 |
| B | 38, 98, 120, 181, 182, 288, 401, 469, 529, 593, 615, 787, 814, 904, 1025, 1077, 1138, 1143, 1195, 1257, 1292, 1402, 1416, 1433, 1444, 1457, 1461, 1639, 2855, 2893, 2939, 2995, 3040, 3063, 3103, 3572 |
| C | 33, 135, 186, 191, 237, 315, 450, 537, 570, 600, 617, 786, 808, 930, 985, 1070, 1096, 1124, 1191, 1262, 1316, 1394, 1408, 1414, 1457, 1461, 1479, 1612, 2861, 2896, 2896, 2969, 2970, 3020, 3174, 3568 |
| D | 33, 104, 159, 193, 209, 299, 506, 529, 553, 613, 717, 763, 930, 970, 1042, 1099, 1142, 1159, 1213, 1317, 1387, 1424, 1435, 1449, 1457, 1466, 1521, 1581, 2867, 2918, 2928, 2987, 3025, 3049, 3053, 3543 |
| TSAB | 2303i, 89, 108, 173, 213, 416, 422, 548, 563, 683, 804, 849, 906, 962, 1067, 1142, 1157, 1161, 1177, 1207, 1288, 1398, 1409, 1431, 1445, 1453, 1457, 1544, 1667, 2908, 2935, 2953, 2953, 3035, 3038, 3062 |
| TSAC | 2556i, 13, 168, 199, 226, 391, 411, 581, 596, 633, 778, 907, 953, 989, 1065, 1095, 1107, 1132, 1132, 1251, 1305, 1388, 1402, 1410, 1450, 1462, 1467, 1509, 1682, 2877, 2893, 2913, 2964, 2970, 2975, 3090 |
| TSBC | 2261i, 93, 179, 299, 404, 437, 495, 536, 593, 634, 649, 755, 825, 949, 998, 1068, 1088, 1111, 1146, 1189, 1235, 1307, 1340, 1406, 1411, 1430, 1472, 1496, 1605, 2866, 2922, 2949, 2981, 3031, 3090, 3590 |
| TSCD | 2355i, 86, 176, 207, 218, 431, 435, 558, 616, 638, 711, 780, 824, 937, 999, 1059, 1074, 1087, 1128, 1199, 1268, 1314, 1392, 1401, 1449, 1454, 1515, 1558, 1628, 2879, 2940, 2948, 2970, 2987, 3100, 3506 |
| $C_2H_5CO^+$ | 192, 194, 401, 560, 703, 751, 879, 1058, 1097, 1237, 1274, 1398, 1399, 1452, 1454, 2329, 2883, 2900, 2936, 2985, 2986 |
| $CH_3O^\bullet$ | 730, 990, 1082, 1414, 1423, 1487, 2842, 2901, 2918 |
| $CH_3O^\bullet$ [b] | 595(2), 660, 1315, 1407(2), 2962(2), 3079 |
| TS[c] | 11, 52, 64, 76, 101, 730, 990, 1082, 1414, 1423, 1487, 2842, 2901, 2918, 192, 194, 401, 560, 703, 751, 879, 1058, 1097, 1237, 1274, 1398, 1399, 1452, 1454, 2329, 2883, 2900, 2936, 2985, 2986 |

[a] Scaled by 0.8929 HF/6-31g* frequencies.[21] Transition state imaginary frequencies denoted (i). Degeneracies listed in parentheses. [b] Experimentally determined frequencies.[32,33] [c] $CH_3O^\bullet$ loss transition state.

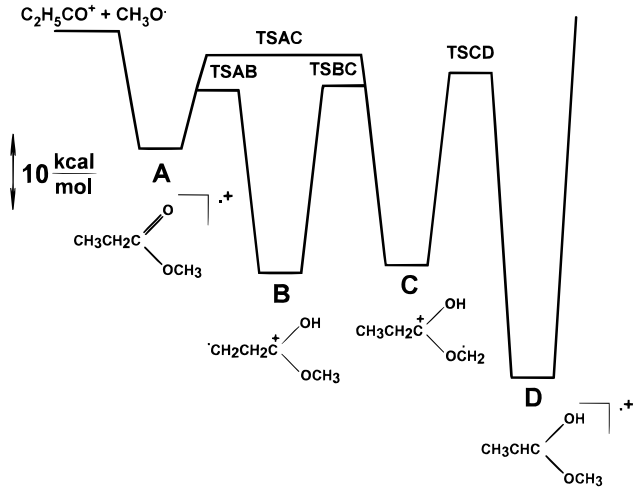


**Figure 2.** Hypersurface for the rearrangement and dissociation reactions of the methyl propionate ion. This diagram is approximately to scale.

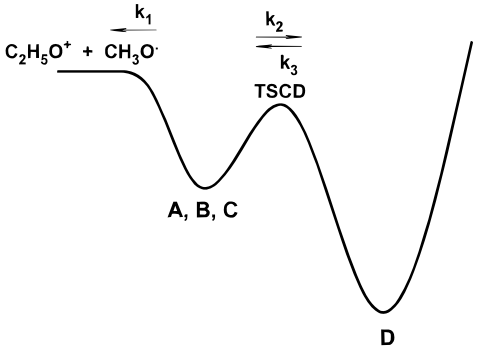


**Figure 3.** Two-well one-product model potential energy surface for the dissociation/isomerization of the ionized methyl propionate. The methyl propionate ion A and the two distonic isomers B and C are combined into a single well.

Figure 3. This model predicts two-component dissociation rates for the methyl propionate ions. The fast component arises from the dissociation via the $CH_3O^\bullet$ loss from the combined potential energy well A, B, C (see Figure 3). In competition with this dissociation is isomerization to the enol ion well D. The slow dissociation rate arises from the slow back-reaction.

It should be noted that the energies obtained by the ab initio MO calculations are not sufficiently precise to permit their use without some adjustment in modeling the statistical theory fit to the experimental rate constants. We thus present calculations as a starting point and permit adjustments of ±3 kcal/mol. On the other hand, we choose to use the vibrational frequencies of

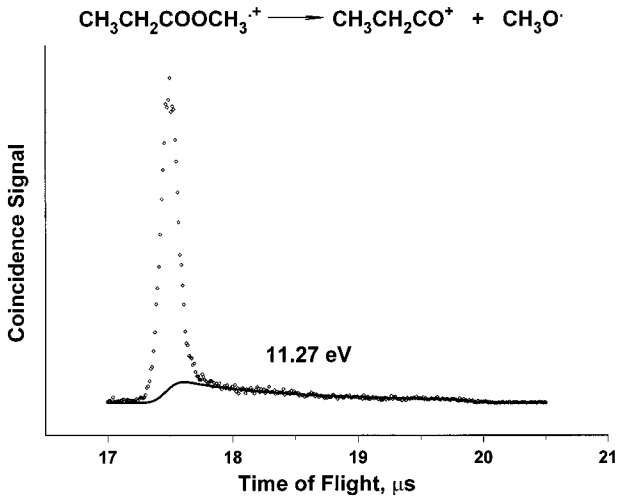


**Figure 4.** Coincidence mass spectra (diamonds) of the room-temperature sample of methyl propionate. The solid line is a calculated TOF distribution of the fragment propanoyl ions resulting from the slow dissociation of the ionized methyl propionate modeled by application of the internal energy distribution function in Figure 5 to the slow dissociation rate curve shown in Figure 7.

the stable isomers of the methyl propionate and the transition states linking them as given by the HF/6-31g* calculations (see Table 2).

### Experimental Results

The TPEPICO TOF mass spectra of methyl propionate were collected over the photon energy range 11.11−11.44 eV. A typical TOF distribution of the fragment propanoyl ion is shown in Figure 4. The fragment ion peaks are two-component, consisting of the narrow (fwhm ≈ 170 ns) symmetric part and the long asymmetric tail which extends up to 20 $\mu$s. The asymmetric part is due to molecular ions dissociating slowly in the first acceleration region of the mass spectrometer, when their average lifetime is comparable to the time it takes them to traverse the first acceleration region (6.7 $\mu$s). The sharp symmetric peak corresponds to the ions dissociating on the time scale less than $10^{-7}$ s, that is, largely to those ions that undergo a direct bond cleavage reaction with the loss of the methoxy radical. The asymmetric part of the fragment ion TOF distribution corresponds to those methyl propionate ions that undergo isomerization reactions to the lower energy structures. The parent ion peak (not shown in Figure 4) consists of both the undissociated methyl propionate ions and those ions that decay in the drift region of the mass spectrometer. In the rate analysis described here, we take this into account.

In the second experiment performed, the adiabatic ionization energy (IE) of methyl propionate was obtained by plotting the normalized molecular ion peak area versus photon energy near the threshold for its observation. The onset energy was determined to be 10.03 ±0.05 eV. Holmes and Lossing[12] and Traeger[10] reported a somewhat higher IE value of 10.15 eV. This IE is extremely difficult to determine because of the significant change in the molecular geometry upon ionization which results in a slowly rising ion signal near the ionization threshold.

**Data Analysis.** As expected from the ab initio MO calculations, we have found that the TOF distributions of the fragment propanoyl ions (see Figure 4) cannot be modeled using a single dissociation rate constant. The broad rovibrational thermal energy distribution of the methyl propionate ions (see Figure 5) and the broad distribution of the dissociation rate constants

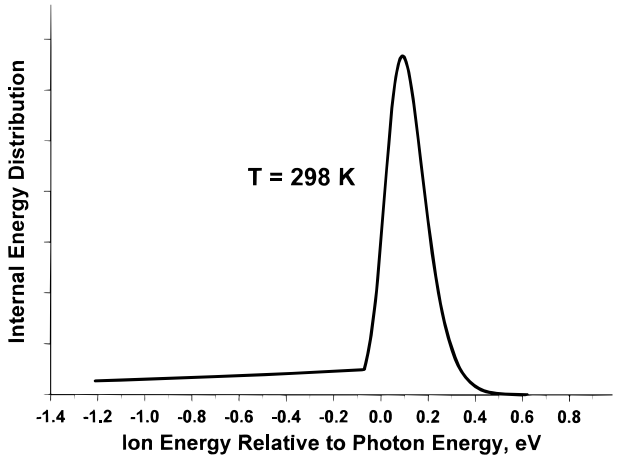


**Figure 5.** Methyl propionate ion rovibrational energy distribution, obtained by convolution of the sample thermal energy distribution with the electron energy analyzer function. Zero on the abscissa corresponds to the photon energy.

associated with it cannot account for the symmetric part of the fragment ion peaks, as in the case of the methyl butanoate and methyl 2-methyl butanoate ions.[13,24] To determine the ratio between the fast and slow dissociation components in the propanoyl ion TOF peak, the symmetric part of the fragment ion's spectrum was approximated by a Gaussian function and the area below this function was related to the area of the rest of the ion's TOF distribution, including the molecular ion peak. The ratio $R$ of the fast dissociation component to the slow dissociation component as a function of the photon energy is shown in Figure 6.

For the simple two-well model shown in Figure 3, the expression for the ratio $R$ is given by eq 1

$$R(E) = \frac{k_1(E)}{k_2(E)} \tag{1}$$

where the $E$ is a molecular ion energy relative to the energy of the dissociation products, $CH_3CH_2CO^+ + CH_3O^\bullet$. This can be written as

$$R(E) = \frac{N^{\ddagger}(E)}{N^{\ddagger}_{\mathrm{TSCD}}(E - \Delta E_{\mathrm{TSCD}})} \tag{2}$$

where $N^{\ddagger}(E)$ and $N^{\ddagger}_{\mathrm{TSCD}}(E - \Delta E_{\mathrm{TSCD}})$ are the sums of states of the transition state for the $CH_3O^\bullet$ loss reaction and the transition structure TSCD at the energy $E$, respectively, and $\Delta E_{\mathrm{TSCD}}$ is the energy of TSCD relative to the reaction products (negative value).

The formula for the slow dissociation rate constant, $k_{\mathrm{slow}}$, in terms of the rate constants $k_1$, $k_2$, and $k_3$ (see Figure 3) is given by eq 3

$$k_{\mathrm{slow}}(E) = \frac{k_1(E)}{k_1(E) + k_2(E)} k_3(E) \tag{3}$$

By substituting the rate constants $k_1$, $k_2$, and $k_3$ with the corresponding RRKM expressions, we note that

$$k_{\mathrm{slow}}(E) = \frac{N^{\ddagger}(E)}{N^{\ddagger}(E) + N^{\ddagger}_{\mathrm{TSCD}}(E - \Delta E_{\mathrm{TSCD}})} \frac{\sigma N^{\ddagger}_{\mathrm{TSCD}}(E - \Delta E_{\mathrm{TSCD}})}{h\rho_{\mathrm{D}}(E - \Delta E_{\mathrm{D}})} \tag{4}$$

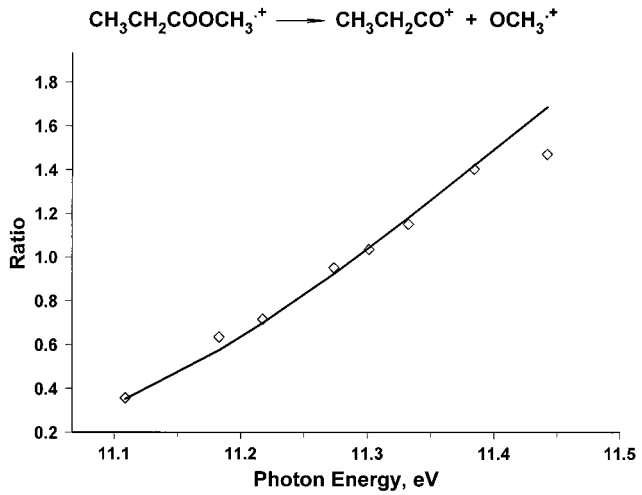


**Figure 6.** Ratio of the fast dissociation component area to the slow dissociation component area in the methyl propionate ion TOF spectra (diamonds) and its best fit (solid line) modeled with the two-well PES taking into account the thermal energy distribution of the methyl propionate ions shown in Figure 5 vs photon energy.

where $h$ is the Plank's constant, $\sigma$ is the reaction degeneracy, which in this case is 1, $\Delta E_D$ is the energy of the enol isomer D with respect to the dissociation products, and $\rho(E - \Delta E_D)$ is a density of states of the enol ion D at the energy $E$ relative to the reaction products.

Because the isomerization processes, C → D and D → C, involve the hydrogen transfer and are thus subjected to tunneling, $N^{\ddagger}_{TSCD}(E - \Delta E_{TSCD})$ must be calculated using the tunneling correction to the transition structure's number of states:[25]

$$N^{\ddagger}_{TSCD}(E - \Delta E_{TSCD}) = \int_{E_C - \Delta E_{TSCD}}^{E - \Delta E_{TSCD}} \kappa(\epsilon)\, \rho^{\ddagger}(E - \Delta E_{TSCD} - \epsilon)\, d\epsilon \quad (5)$$

In this expression, $\epsilon_t$ is the translational energy in the reaction coordinate, $\kappa(\epsilon_t)$ is the tunneling probability, $\rho^{\ddagger}$ is the density of states of the transition state TSCD, and $E_C$ is the relative energy of the distonic isomer C with respect to the dissociation products (again, the negative value). Thus, the isomerization barrier for the structure C can be expressed as $-E_C + \Delta E_{TSCD}$. The tunneling probability can be calculated using the Eckart model of the barrier[26] as described by Baer and Hase.[8]

With the molecular ion internal energy deposition function (see Figure 5) prepared as described by Keister et al.[27] and eq 2 in hand, the energy dependence of the ratio of fast to slow dissociation components in the methyl propionate ion's TOF distributions (see Figure 6) can be modeled using the relative energy of the transition state TSCD with respect to the dissociation products, $\Delta E_{TSCD}$, as the adjustable parameter. While the vibrational frequencies of the transition state TSCD were given by the ab initio MO calculations (see Table 2), the set of frequencies of the $CH_3O^{\bullet}$ loss transition state, however, was guessed. The loss of the methoxy radical from the methyl propionate ion proceeds without a reverse barrier so that the variational transition state theory (VTST)[8,28,29] should be used. However, given the amount of averaging needed to analyze the data, we chose not to use the VTST here. Rather, we simply used the combined set of vibrational frequencies for the propanoyl ion and methoxy radical (see Table 2) and added five low modes (from 10 to 100 $cm^{-1}$) in order to fit the slope of the $R(E)$ function (see Figure 6). These are frequencies which turn into product rotations and thus are reduced to zero as the ion proceeds toward products. These added frequencies are quite low, which is consistent with a loose transition state. The data in Figure 6 are quite sensitive to these low modes, and even a 10% change in them would lead to a poorer fit.

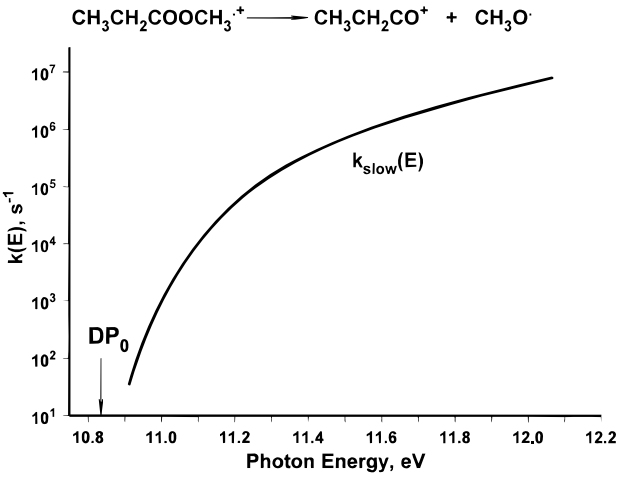


**Figure 7.** Experimentally derived slow dissociation rate constant for the $CH_3O^{\bullet}$ loss reaction of ionized methyl propionate.

Modeling of the ratio was performed simultaneously with the modeling of the asymmetric part of the TOF distributions (see Figure 4), that is, the slow dissociation component. The TOF distribution of slowly dissociating ions was calculated using the rate constant given by eq 4 and the energy deposition function shown in Figure 5 as described by Keister et al.[27] To fit the asymmetric part of the fragment ion TOF distribution, the energy of the enol isomer D with respect to the dissociation products,$\Delta E_D$, was varied.

From the best fits of the ratio of the fast to slow dissociation components in the methyl propionate ion's TOF distributions and the asymmetric part of the fragment ion TOF peaks shown by solid lines in Figures 4 and 6, respectively, the relative energies of the transition state TSCD and the enol ion $CH_3CHC(OH)OCH_3^{\bullet+}$ with respect to the reaction products, $CH_3CH_2CO^+$ and $CH_3O^{\bullet}$, were found to be −0.430 and −2.015 eV, respectively. Variation of these values by 10 meV resulted in significantly worse fits to the data in Figures 4 and 6. The fit to the slow dissociation component in the propanoyl ion TOF distributions was made using the $k_{slow}(E)$ curve (see eq 4) shown in Figure 7.

**Derived Thermochemical Data.** As shown in Table 3, the adiabatic IE of the methyl propionate is 10.03 ± 0.05 eV. If we combine this with the 0 K heat of formation of the neutral methyl propionate of −97.4 kcal/mol, obtained by converting the 298 K value of −103.3 kcal/mol (estimated by Holmes and Lossing[12] from group additivity methods), we obtain a 0 K heat of formation of the methyl propionate ion of 134 kcal/mol. We arbitrarily assign an uncertainty of ±2 kcal/mol to this value. The molecular mechanics calculations (MMX)[30] yielded the $\Delta H^0_{f(298K)}$ ($CH_3CH_2COOCH_3$) of −100 kcal/mol, which agrees within the combined errors of the MMX and the Holmes estimation. The 0 K heat of formation of the enol isomer of the methyl propionate ion, $CH_3CHC(OH)OCH_3^{\bullet+}$, was found to be equal to 106 ± 2 kcal/mol in our previous work.[13] This value is in good agreement with the value of 105 kcal/mol obtained by converting the Holmes and Lossing 298 K value of 99 kcal/mol.[12] Thus, the keto form of the methyl propionate ion is 28 kcal/mol less stable than its enol tautomer (see structures A and D in Figure 1).[13] This value is in good agreement with both the

**TABLE 3: Experimental Energies of Relevant Species**

| species | $\Delta H_{f(0K)}$ (neutral), kcal/mol | $\Delta H_{f(0K)}$ (ion), kcal/mol | IE/DP, eV |
|---|---|---|---|
| $CH_3CH_2COOCH_3$ | $-97.4 \pm 2$[a] | $134 \pm 2$[b]<br>137[c] | $10.03 \pm 0.05$[b]<br>10.15[10, 12] |
| $CH_3CHCOHOCH_3$ | | $106 \pm 2$[13]<br>105[d] | |
| $CH_3CH_2CO^+$ | | $147 \pm 2$[b] | $10.83 \pm 0.01$[b]<br>10.78[e] |
| $CH_3O^\bullet$ | $5.4 \pm 0.7$[f] | | |

[a] The 0 K heat of formation of the methyl propionate was obtained by converting the 298 K value of $-103.3$ kcal/mol[12] using the HF/6-31g* vibrational frequencies (see Table 2). [b] The 0 K values obtained in the present work. [c] The 0 K heat of formation of the methyl propionate ion was derived using the Holmes and Lossing value of IE.[12] [d] The 0 K heat of formation of the enol ion of the methyl propionate was obtained by converting the 298 K value of 99 kcal/mol[12] using the HF/6-31g* vibrational frequencies (see Table 2). [e] The 298 K value.[10] [f] The 0 K heat of formation of the methoxy radical was obtained by converting the 298 K value of $3.7 \pm 0.7$ kcal/mol[31] using the experimentally determined frequencies[32,33] (see Table 2).

MP2 value of 27.5 kcal/mol and the G2 value of 26.2 kcal/mol (see Table 1).

On the other hand, if we combine the activation energy of the $CH_3O^\bullet$ loss reaction measured from the bottom of the enol ion D well, $-\Delta E_D$, of 2.015 eV with the $\Delta H^0_{f(0K)}$ ($CH_3CHC(OH)OCH_3^{\bullet+}$) of $106 \pm 2$ kcal/mol[13] and the 0 K heat of formation of the methoxy radical of 5.4 kcal/mol, which was obtained by converting the literature value at 298 K of $3.7 \pm 0.7$ kcal/mol[31] using the experimental vibrational frequencies,[32,33] we obtain the 0 K heat of formation of the propanoyl cation of 147 kcal/mol. This value is 2.5 kcal/mol higher than the one obtained by converting the 298 K value of 141.3 kcal/mol reported by Traeger.[10]

The dissociative photoionization threshold for the methyl propionate, $DP_0$, can be calculated using the following expression

$$DP_0 = \Delta H^0_{f(0K)}(CH_3CHC(OH)OCH_3^{\bullet+}) - \Delta H^0_{f(0K)}(CH_3CH_2COOCH_3) - \Delta E_D \quad (6)$$

Equation 6 yields the 0 K value of $DP_0$ of 10.83 eV. If we subtract the adiabatic IE of methyl propionate from this value, we obtain the activation energy of the $CH_3O^\bullet$ loss reaction from the methyl propionate ion, $E_0$, of 18.4 kcal/mol. This value is in very good agreement with the MP2 value of 18.24 kcal/mol but is some 3.3 kcal/mol lower than the G2 value (see Table 1).

Finally, if we combine $E_0$ with the relative energy of the transition state TSCD with respect to the dissociation products, $\Delta E_{TSCD}$, of $-0.430$ eV, we obtain the energy of TSCD relative to the methyl propionate ion of 8.5 kcal/mol, which is in very good agreement with the G2 value (see Table 1).

**Acknowledgment.** We thank the Department of Energy for continuing financial support and the North Carolina Supercomputing Facility for the generous allotment of computer time.

## References and Notes

(1) Mazyar, O. A.; Baer, T. *J. Phys. Chem. A* **1998**, *102*, 1682.
(2) Mazyar, O. A.; Mayer, P. M.; Baer, T. *Int. J. Mass Spectrom. Ion. Processes* **1997**, *167/168*, 389.
(3) Baer, T.; Mazyar, O. A.; Keister, J. W.; Mayer, P. M. *Ber. Bunsen-Ges. Phys. Chem.* **1997**, *101*, 478.
(4) Holmes, J. L.; Hop, C. E. C. A.; Terlouw, J. K. *Org. Mass Spectrom.* **1986**, *21*, 776.
(5) Burgers, P. C.; Holmes, J. L.; Hop, C. E. C. A.; Terlouw, J. K. *Org. Mass Spectrom.* **1986**, *21*, 549.
(6) Laderoute, K. Ph.D. Thesis, University of Toronto, 1984.
(7) Pakarinen, J. M. H.; Vainiotalo, P.; Stumpf, C. L.; Leeck, D. T.; Chou, P. K.; Kenttämaa, H. I. *J. Am. Soc. Mass Spectrom.* **1996**, *7*, 482.
(8) Baer, T.; Hase, W. L. *Unimolecular Reaction Dynamics: Theory and Experiments*; Oxford University Press: New York, 1996.
(9) Yates, B. F.; Radom, L. *J. Am. Chem. Soc.* **1987**, *109*, 2910.
(10) Traeger, J. C. *Org. Mass Spectrom.* **1985**, *20*, 223.
(11) Leeck, D. T.; Stirk, K. M.; Zeller, L. C.; Kiminkinen, L. K. M.; Castro, L. M.; Vainiotalo, P.; Kenttämaa, H. I. *J. Am. Chem. Soc.* **1994**, *116*, 3028.
(12) Holmes, J. L.; Lossing, F. P. *J. Am. Chem. Soc.* **1980**, *102*, 1591.
(13) Mazyar, O. A.; Baer, T. *J. Am. Soc. Mass Spectrom.*, in press.
(14) Baer, T.; Booze, J. A.; Weitzel, K. M. In *Vacuum ultraviolet photoionization and photodissociation of molecules and clusters*; Ng, C. Y., Ed.; World Scientific: Singapore, 1991; p 259.
(15) Baer, T.; Lafleur, R.; Mazyar, O. In *Energetics of Stable and Reactive Intermediates*; Minas da Piedade, M., Ed.; Kluwer Academic Publishers: Dordrecht, Netherlands, in press.
(16) Curtiss, L. A.; Raghavachari, K.; Trucks, G. W.; Pople, J. A. *J. Chem. Phys.* **1991**, *94*, 7221.
(17) Weitzel, K. M.; Booze, J. A.; Baer, T. *Chem. Phys.* **1991**, *150*, 263.
(18) Baer, T.; Peatman, W. B.; Schlag, E. W. *Chem. Phys. Lett.* **1969**, *4*, 243.
(19) Spohr, R.; Guyon, P. M.; Chupka, W. A.; Berkowitz, J. *Rev. Sci. Instrum.* **1971**, *42*, 1872.
(20) Frisch, M. J.; Trucks, G. W.; Schlegel, H. B.; Gill, P. M. W.; Johnson, B. G.; Robb, M. A.; Cheeseman, J. R.; Keith, T.; Petersson, G. A.; Montgomery, J. A.; Raghavachari, K.; Al-Laham, M. A.; Zakrzewski, V. G.; Ortiz, J. V.; Foresman, J. B.; Cioslowski, J.; Stefanov, B. B.; Nanayakkara, A.; Challacombe, M.; Peng, C. Y.; Ayala, P. Y.; Chen, W.; Wong, M. W.; Andres, J. L.; Replogle, E. S.; Gomperts, R.; Martin, R. L.; Fox, D. J.; Binkley, J. S.; Defrees, D. L.; Baker, J.; Stewart, J. P.; Head-Gordon, M.; Gonzalez, C.; Pople, J. P. *Gaussian 94*, revision D.1; Gaussian, Inc.: Pittsburgh, PA, 1995.
(21) Pople, J. A.; Scott, A. P.; Wong, M. W.; Radom, L. *Isr. J. Chem.* **1993**, *33*, 345.
(22) Scott, A. P.; Radom, L. *J. Phys. Chem.* **1996**, *100*, 16502.
(23) Heinrich, N.; Schmidt, J.; Schwarz, H.; Apeloig, Y. *J. Am. Chem. Soc.* **1987**, *109*, 1317.
(24) Mazyar, O. A.; Baer, T. *Int. J. Mass Spectrom. Ion. Proc.*, in press.
(25) Miller, W. H. *J. Am. Chem. Soc.* **1979**, *101*, 6810.
(26) Eckart, C. *Phys. Rev.* **1930**, *35*, 1303.
(27) Keister, J. W.; Tomperi, P.; Baer, T. *Int. J. Mass Spectrom. Ion. Processes* **1997**, *171*, 243.
(28) Truhlar, D. G.; Garrett, B. C. *Acc. Chem. Res.* **1980**, *13*, 440.
(29) Hase, W. L. *J. Chem. Phys.* **1976**, *64*, 2442.
(30) *PCMODEL for Windows*; Serena Software: Bloomington, IN, 1994. The MMX force field is an extension of N. L. Allinger's MM2 (QCPE-395, 1977) force field and includes pi routines from his MMP1 (QCPE-318). These are available from the Quantum Chemistry Program Exchange, Creative Arts Building 181, 840 State Highway 46 Bypass, Bloomington, IN 47405, Programs 395 and 318. Changes were made by J. J. Gajewski and K. E. Gilbert, 1994.
(31) Lias, S. G.; Bartmess, J. E.; Liebman, J. F.; Holmes, J. L.; Levin, R. D.; Mallard, W. G. *Gas Phase Ion and Neutral Thermochemistry*, *J. Phys. Chem. Ref. Data*; NSRDS: U.S. Government Printing Office: Washington, DC, 1988; Vol. 17, suppl. 1.
(32) Foster, S. C.; Misra, P.; Lin, T.-Y.; Damo, C. P.; Carter, C. C.; Miller, T. A. *J. Phys. Chem.* **1988**, *92*, 5914.
(33) Jacox, M. E. *J. Phys. Chem. Ref. Data.* **1990**, *19*, 1387.